Fundus Near Infrared Fluorescence Correlates with Fundus Near Infrared Reflectance

Andreas W. A. Weinberger,[1] *Alexandra Lappas,*[2] *Thomas Kirschkamp,*[1] *Babac A. E. Mazinani,*[1] *Julia K. Huth,*[1] *Babak Mohammadi,*[1] *and Peter Walter*[1]

Purpose. To analyze the occurrence of near infrared (NIR) fluorescence in relation to NIR reflectance, blue-light–excited autofluorescence, angiograms, and funduscopy.

Methods. Observational consecutive case series in patients with macular diseases. Imaging was performed with a confocal scanning laser ophthalmoscope for NIR reflectance, blue-light–excited autofluorescence, NIR fluorescence, and fluorescein and indocyanine green (ICG) angiograms. In cases in which NIR fluorescence was observed, five to nine images were averaged. The leakage of the scanning laser ophthalmoscope was analyzed.

Results. In the 291 eyes analyzed, NIR fluorescence was observed in 51 and was graded weak in 27 with wet age-related macular degeneration (AMD, 10 cases), dry AMD with pigment clumping ($n = 7$), chronic central serous choroidopathy (CSC; $n = 5$), choroidal nevi ($n = 2$), subretinal hemorrhages ($n = 2$), and chloroquine maculopathy ($n = 1$). Strong NIR fluorescence was found in 24 eyes, with wet AMD ($n = 14$), subretinal hemorrhages ($n = 8$), and choroidal nevi ($n = 2$). Except for four eyes, we observed a strong correlation of NIR fluorescence and increased NIR reflectance at identical fundus location (92.2%). NIR fluorescence corresponded with increased blue-light–excited autofluorescence in 21 of 31 patients with AMD and in 4 of 5 patients with chronic CSC, but in none of the 4 patients with nevi. Funduscopy showed that structures with NIR fluorescence were pigmented or consisted of degraded blood. Barrier filter leakage of the imaging system was 6.2×10^{-6}.

Conclusions. The high correlation of NIR fluorescence and reflectance indicated that part of the observed NIR fluorescence is pseudofluorescence, whereas gray-scale analysis indicated that both NIR autofluorescence and pseudofluorescence contribute to the NIR fluorescence images. Quantification of leakage of the imaging system indicated a significant part of the observed NIR fluorescence is NIR autofluorescence. As NIR fluorescence derives from pigmented lesions, melanin is a possible source if NIR reflectance is also increased. Comparison with blue-light–excited autofluorescence showed differences between AMD and patients with nevi. NIR autofluorescence was also detected in single cases of maculopathy without corresponding NIR reflectance. (*Invest Ophthalmol Vis Sci.* 2006;47:3098–3108) DOI:10.1167/iovs.05-1104

Angiograms using the dyes sodium fluorescein and indocyanine green (ICG) are standard tools in the diagnosis of retinal and choroidal disease. Modern angiography systems include confocal scanning laser ophthalmoscopes which allow high-resolution imaging at different wavelengths. Preinjection fluorescence has been observed in fluorescein angiograms and ICG angiograms. However, one must distinguish between pseudofluorescence and autofluorescence. The former describes light reflected from fundus structures that bypasses the barrier filter of the angiography system, whereas autofluorescence describes natural fluorescence emitted from fluorescent fundus structures, the excitation and emission spectra of which lie in the range of the fluorescent dyes used for angiography. Several natural fluorophores, such as lipofuscin (Delori FC, et al. *IOVS* 1994;35:ARVO Abstract 2145),[1] have been described to emit light in a broad range of wavelengths. Lipofuscin fluorescence occurs between 500 and 750 nm with a peak emission of ~630 nm. Optic nerve head drusen and astrocytic hamartoma also fluoresce. Analysis of fundus lipofuscin using the images of fundus autofluorescence more than 505 nm in patients with age-related macular degeneration (AMD) has become a widely used tool in retina centers.[2–4]

Piccolino et al.[5] screened 450 patients and detected ICG preinjection fluorescence at 815 nm in 40.8% of their patients using a video-based imaging system (IMAGEnet H1024 digital imaging system; Topcon, Tokyo, Japan). In their paper, the authors discussed whether the observed ICG preinjection fluorescence is pseudofluorescence or autofluorescence. As highly reflective fundus structures such as bare sclera did not show preinjection fluorescence, the authors interpreted their observation as autofluorescence.

Recently, analysis of ICG preinjection fluorescence has become a tool for follow-up examinations in patients who have undergone ICG-assisted macular surgery. However, in these cases, fluorescence of ICG remnants are observed that remain in the eye for long periods.[6,7] Infrared (IR) imaging has been described as particularly advantageous in identifying subretinal structures[8] and improving the discrimination between choroidal hemorrhage and choroidal melanoma.[9]

In this study, we investigated the incidence of ICG preinjection fluorescence, which we termed near infrared (NIR) fluorescence, its relation to NIR reflectance, blue light–excited autofluorescence and funduscopy.

Methods

Patients scheduled for angiography for various macular disorders were included in the study when optic media were clear, and the pupil

From the [1]Department of Ophthalmology, RWTH Aachen University, Aachen, Germany; and the [2]Center for Ophthalmology, Department of Vitreoretinal Surgery and Retinal Disease, University of Cologne, Cologne, Germany.

Presented at the annual meeting of the Association for Research in Vision and Ophthalmology, Fort Lauderdale, Florida, May 2005, and at the joint meeting of the 102nd German Ophthalmological Society annual meeting and 15th European Society of Ophthalmology Congress, Berlin, Germany, September 2005.

Supported in part by Deutsche Forschungsgemeinschaft (DFG) Priority Research Program SPP1088.

Submitted for publication August 21, 2005; revised February 4 and March 18, 2006; accepted May 19, 2006.

Disclosure: **A.W.A. Weinberger**, None; **A. Lappas**, None; **T. Kirschkamp**, None; **B.A.E. Mazinani**, None; **J.K. Huth**, None; **B. Mohammadi**, None; **P. Walter**, None

The publication costs of this article were defrayed in part by page charge payment. This article must therefore be marked "*advertisement*" in accordance with 18 U.S.C. §1734 solely to indicate this fact.

Corresponding author: Andreas W. A. Weinberger, RWTH Aachen University, Department of Ophthalmology, Pauwelsstr. 30, D-520744 Aachen, Germany; aweinberger@ukaachen.de.

dilated to at least 5 mm. Imaging was performed with a scanning laser ophthalmoscope (HRA Classic; Heidelberg Engineering, Dossenheim, Germany) using the 30° field of view and 512 × 512 pixel resolution. NIR fluorescence imaging and ICG angiograms used a diode laser at 787 nm for excitation and a barrier filter allowing light passage >810 nm. The product of barrier filter transmission and output coupler reflectance determines the leakage of an imaging system. To quantify leakage of the barrier filter and off-band emission from the NIR laser, a spectral analysis (spectrometer USB 2000 VIS-NIR; Ocean Optics BV, Duiven, The Netherlands) of laser light was performed directly from the diode after gray filter laser power reduction and after passing the barrier filter and the HRA optics. In addition, NIR laser power (Powermeter Nova, sensor head PD-300; Ophir Optronics Ltd., Jerusalem, Israel) was measured at the lens aperture of the scanning laser ophthalmoscope, at the laser fiber, and after barrier filter passage to determine barrier filter transmission. The reflectance of the output coupler was determined for s- and p-polarized laser light. For NIR fluorescence imaging, the scanning laser ophthalmoscope was switched into ICG-angiography mode, and gain was increased until the optic disc and retinal vessels became just visible, as described for blue light autofluorescence imaging in fluorescein angiography mode.[4] For NIR fluorescence and blue light autofluorescence, five to nine images at 512 × 512 pixel resolution were taken and averaged using the HRA mean algorithm supplied. This algorithm normalizes gray values from 0 to 255, which produces enhanced image quality but does not allow gray-value analysis in the resultant normalized image. In cases where the brightest area in an NIR reflectance image was not in saturation and the corresponding NIR fluorescence raw data image showed a signal, gray-value analysis was performed in raw-data images before normalizing with the HRA software tool to compare NIR reflectance and NIR fluorescence ratios compared with background. NIR fluorescence was rated as strong if a clear area of increased NIR fluorescence was visible in a single frame (gray-value ratio for area of interest/neighboring area >1.5), whereas NIR fluorescence was rated weak if a clear signal was seen only after averaging (gray-value ratio for area of interest/neighboring area >1.1–1.5). To determine the localization of NIR fluorescence in corresponding NIR reflectance, green-light–, and blue-light–excited autofluorescence images, the distance from the center of the disc was measured with the HRA software tool and pasted into the corresponding image. NIR reflectance imaging was performed at 820 nm with a diode laser. For blue-light–excited autofluorescence imaging and fluorescein angiograms an argon blue laser (488 nm) was used for excitation and a barrier filter with a cutoff of 10^{-6}, allowing light passage of >505 nm.[4] Green-light images were obtained with an argon green laser at 680 nm. Fundus color photographs were taken with a digital fundus camera (F 450 plus; Carl Zeiss Meditec, Jena, Germany) The study protocol adhered to the provisions of the Declaration of Helsinki.

Results

We included 291 eyes (Table 1). NIR fluorescence was observed in 51 (17.5%.) eyes. Fundus images are shown for six cases in Figures 1 through 6 and are shown in composite color photographs in Figure 7. Generally, NIR fluorescence was much weaker than comparable blue-light–excited autofluorescence images. Similar to blue-light–excited autofluorescence, the optic disc and retinal vessels appeared darker than background, but NIR fluorescence did not show the dip in intensity at the fovea caused by macular pigment, as seen in blue-light–excited autofluorescence,[1] but increased slightly toward the macular center. NIR fluorescence was graded weak in 27 (9.3%) eyes with exudative AMD (10 eyes), dry AMD with pigment clumping (7 eyes), chronic central serous choroidopathy (5 eyes), choroidal nevi (2 eyes), subretinal hemorrhages (2 eyes), and chloroquine maculopathy (1 eye). NIR fluorescence was graded strong in 24 eyes (8.2%) with exudative AMD (14 eyes), subretinal hemorrhages (8 eyes), or choroidal nevi (2 eyes). Except for one case of chloroquine maculopathy (Fig. 6) and 3 eyes with chronic CSC (Fig. 4), we observed a strong correlation of NIR fluorescence and increased NIR reflectance at identical fundus locations (92.2%). NIR fluorescence corresponded with increased blue-light–excited autofluorescence in 21 of 31 AMD eyes, 3 of 10 eyes with subretinal hemorrhage (Fig. 4), in 4 of 5 eyes with chronic CSC, but in none of the 4 eyes with nevi (Fig. 5). NIR fluorescence signals were not evident after ICG was injected. Funduscopy showed that most structures with NIR fluorescence were either pigmented or consisted of degraded blood.

In the chloroquine maculopathy case (Fig. 6), homogenous NIR autofluorescence was observed. In a circular area of condensed retinal pigment epithelium which showed slightly increased autofluorescence excited by blue light NIR autofluorescence was also increased. In the corresponding area, in those patients with chronic CSC who had NIR fluorescence without increased NIR reflectance, the signals were located in areas of pigment alteration and exudation.

Gray values of NIR reflectance corresponding to detectable increased NIR fluorescence were often in saturation, even if

Table 1 Distribution of Disease Type and Incidence of Near Infrared Fluorescence (NIR-F)

	n	NIR-F Weak >805 nm [No.]	NIR-F Strong >805 nm [No.]	NIR-R 820 nm [No.]	BL-AF >505 nm [No.]
Dry AMD	87	7 (1.286 ± 0.121)	0 —	7	5
Exsudative AMD	154	10 (1.260 ± 0.044)	14 (1.680 ± 0.126)	24	16
Subretinal hemorrhage	19	2 (1.260 ± 0.113)	8 (1.659 ± 0.098)	10	3
Central serous choroidopathy	24	5 (1.262 ± 0.121)	0 —	2	4
Choroidal nevi	6	2 (1.370 ± 0.134)	2 (1.865 ± 0.134)	4	0
Chloroquine maculopathy	1	1 —	0 —	0	1

NIR-fluorescence was subgrouped into weak NIR-fluorescence if in raw data images the gray-value ratio between an area of NIR fluorescence and background was between 1.1 and 1.5, and was subgrouped as strong NIR-fluorescence if this ratio was >1.5. The mean of this ratio and its standard deviation are displayed. The incidence of increased NIR-reflectance (NIR-R) and blue light excited autofluorescence (BL-AF) at retinal locations of NIR-fluorescence are also shown. The Wilcoxon signed rank test showed no significant difference in ratios of weak or strong NIR-fluorescence in correlation with disease type. Total eyes, 291.

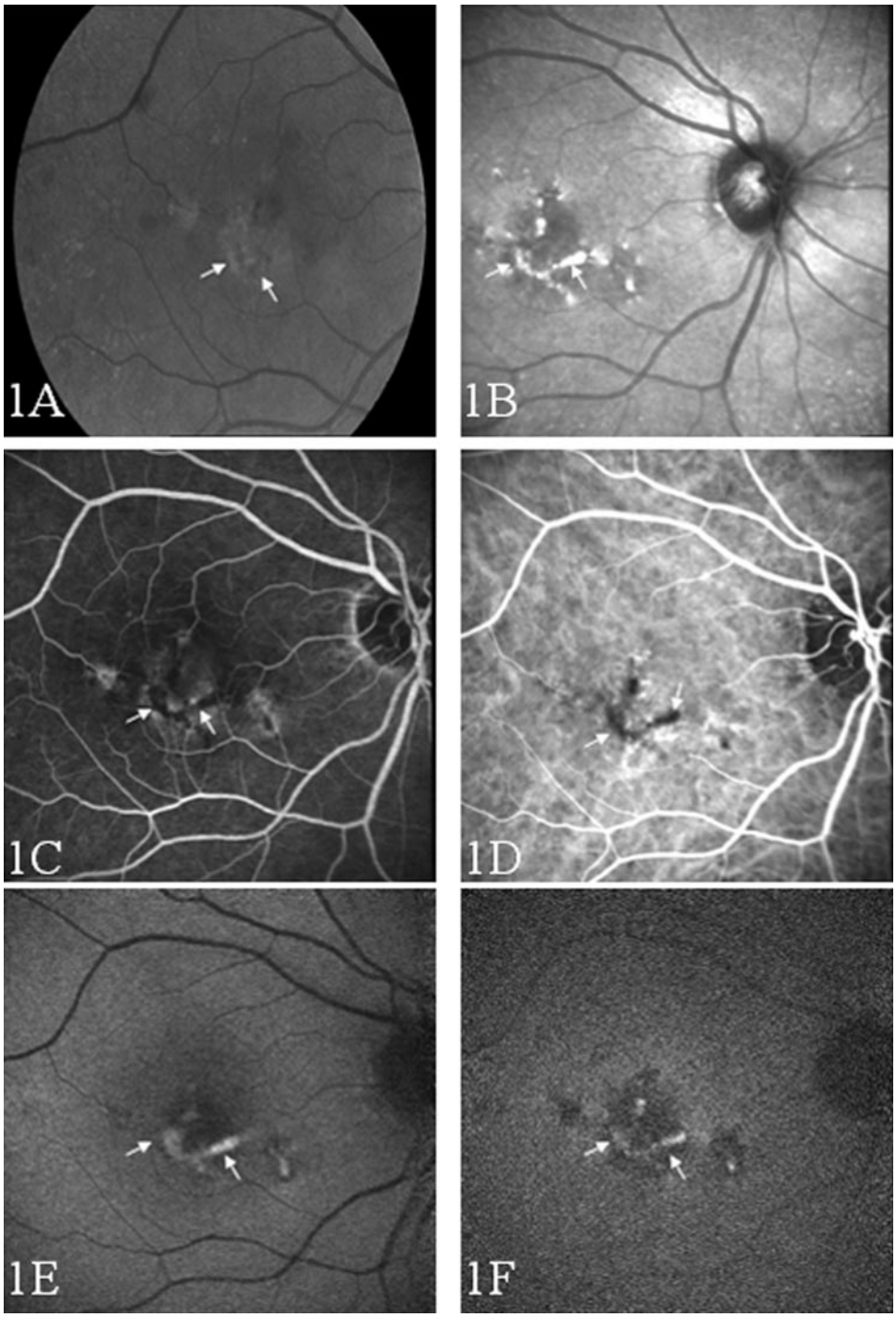

FIGURE 1. Case 1. Pigment condensations in dry AMD/pattern dystrophy: (**A**) fundus photograph, (**B**) NIR reflectance, hyperreflective corresponding to pigmentation (*arrows*) as well as area close to optic disc in saturation. Note that hyperreflective area close to the optic disc does not appear in NIR fluorescence (see **F**) image. (**C**) Fluorescein angiogram. (**D**) ICG angiogram. Note the NIR fluorescence signal (see **F**) does not contribute to the ICG angiogram. (**E**) Blue light excited autofluorescence showing increased autofluorescence corresponding to hyperpigmented lesions. (**F**) NIR fluorescence image, similar to blue-light–excited autofluorescence image (**E**) an increased signal can be observed corresponding to pigmented lesions.

gain was turned down to a minimum, which did not allow gray-value comparison with NIR fluorescence images. Gray-value ratios within IR-reflectance images were stable for varying gain control positions (2.42 ± 0.12) unless these areas did not reach saturation. Of interest, apart from the NIR fluorescence of fundus features, other retinal areas in the same image that also had high NIR reflectance, typically scars or pigment atrophy, did not contribute to the NIR fluorescence (Fig. 6). It seemed these areas had a lower level of reflectance compared with areas showing NIR fluorescence (Fig. 3). In five cases, however, NIR reflectance of fundus diseases showing NIR fluorescence did not reach saturation. In these cases, we compared the ratio of increased NIR reflectance to neighboring reference areas with the corresponding signals in identical areas in the NIR fluorescence image (Fig. 8) to discriminate pseudofluorescence from autofluorescence. In all five cases we observed a higher ratio of NIR fluorescence/reference area than NIR reflectance/NIR reference area.

Analysis of barrier filter leakage for the NIR laser revealed a laser power exiting the scanning laser ophthalmoscope of 2.20 mW for 512×512-pixel normal modulation. The laser power exiting the laser fiber was 8.68 mW, after barrier filter passage 0.105 μW, resulting in a barrier filter transmission of 1.21×10^{-5}. The analysis of laser power after the output-coupling mirror showed a laser power of 2.77 mW for s-polarized laser light (from 8.68 mW exiting the laser fiber) resulting in a

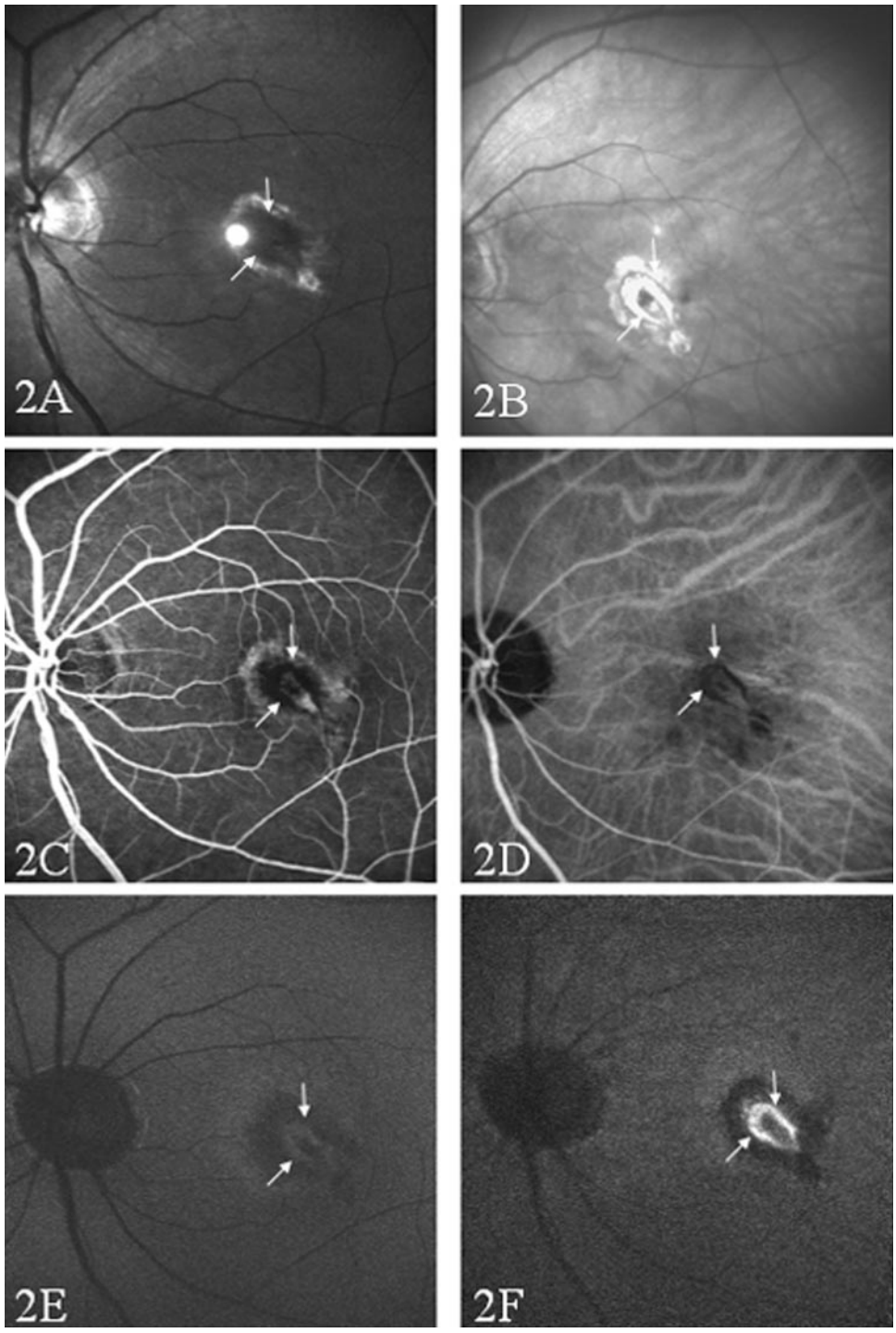

FIGURE 2. Case 2. Pigmented ring around classic choroidal neovascularization 8 weeks after photodynamic therapy (PDT) with verteporfin in AMD. *Arrows*: pigmented oval structure. (**A**) Green-light (red free) image. (**B**) NIR reflectance image. Note both the oval pigmented structure (*arrows*) as well as a surrounding depigmented area are hyperreflective and in saturation. (**C**) Fluorescein angiogram. (**D**) ICG angiogram. (**E**) Slightly increased blue-light–excited autofluorescence can be observed corresponding to the pigmented oval structure. (**F**) NIR fluorescence image. Note the strong signal corresponding to the pigmented oval structure while the surrounding depigmented area is hyporeflective. The strong NIR fluorescence signal does not seem to contribute to fluorescence in the ICG angiogram (**D**).

reflectance of 0.32 for s-polarized laser light. For p-polarized laser light, the laser power after the output coupling mirror was 0.59 mW resulting in a reflectance of 0.07 for p-polarized laser light. After the light passed both the barrier filter and the coupling mirror, we found a remaining laser power of 58 nW for s-polarized laser light and 54 nW for p-polarized laser light, resulting in a leakage of 6.68×10^{-6} for s-polarized and 6.22×10^{-6} for p-polarized laser light for the optical system. The spectral analysis of the emitted laser light exiting the laser fiber revealed no sideband emission (Fig. 9). The spectral analysis after the HRA optics showed a complete suppression of the laser peak, but some sideband emission in the range of 6.2×10^{-6}.

DISCUSSION

Despite preinjection fluorescence at >810 nm being a common finding after ICG-assisted macular surgery,[6,7] its natural occurrence has rarely been described. In our study, we could confirm the observation of preinjection fluorescence in ICG angiography in fundus lesions such as hemorrhages and in pigmented lesions in patients with AMD, as described by Piccolino et al.[5] In contrast to their work, we used a different imaging system (HRA classic; Heidelberg Engineering, Heidelberg, Germany) which uses a confocal aperture and a 6×10^{-6} cutoff with its built in barrier filter. The camera-based system (Topcon) used by Piccolino et al. describes an IR filter peak

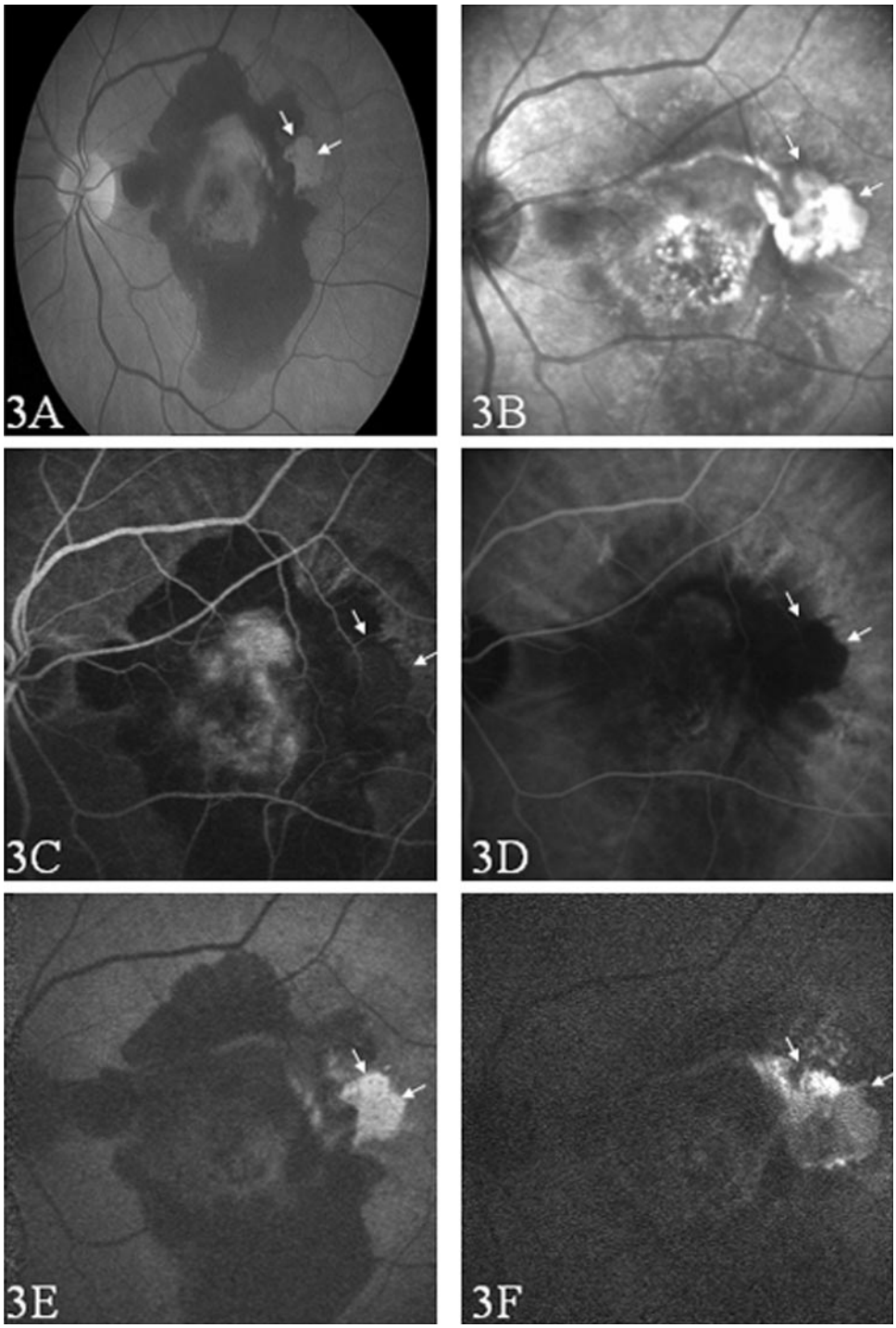

FIGURE 3. Case 3. Subretinal hemorrhage in a patient with exudative AMD. *Arrows*: degraded blood. (**A**) Fundus photograph. (**B**) NIR reflectance. Increased reflectance can be observed corresponding to degraded blood. (**C**) fluorescein angiogram. (**D**) ICG angiogram. (**E**) Increased blue-light–excited autofluorescence can be observed corresponding to degraded blood. (**F**) Strong NIR fluorescence corresponding to increased NIR reflectance seen in (**B**).

with absorption at 805 nm, peak fluorescence at 835 nm, and a filter curve overlap less than 0.5%.[5] With increasing wavelength the fundus reflectance increases and for NIR light, it is approximately 1 log unit higher than visible light.[8] Comparing camera-based systems with confocal scanning laser ophthalmoscopes showed that camera-based systems produces lower IR image quality due to the camera's inability to separate reflected and scattered light.[10]

In addition to technical differences, in our study, the ICG-preinjection fluorescence images we termed NIR fluorescence images were noise reduced by software averaging five to nine single images. Such an averaging is a standard technique to improve image quality of originally weak signals and is in clinical use for blue-light–excited autofluorescence imaging.[4,8,11] In our opinion, the different technical systems used explain the lower overall rate of NIR fluorescence observed in our patient group and probably also explains why we did not observe any persistence of NIR fluorescence after ICG was injected. Observing the high correlation of increased NIR fluorescence and increased NIR reflectance indicated that the observed NIR fluorescence is pseudofluorescence deriving from barrier filter leakage. In contrast, highly NIR-reflective structures such as depigmented areas were successfully blocked by the barrier filter. An explanation is that structures producing NIR fluorescence have a much stronger NIR reflectance than do depigmented areas, and this could be observed

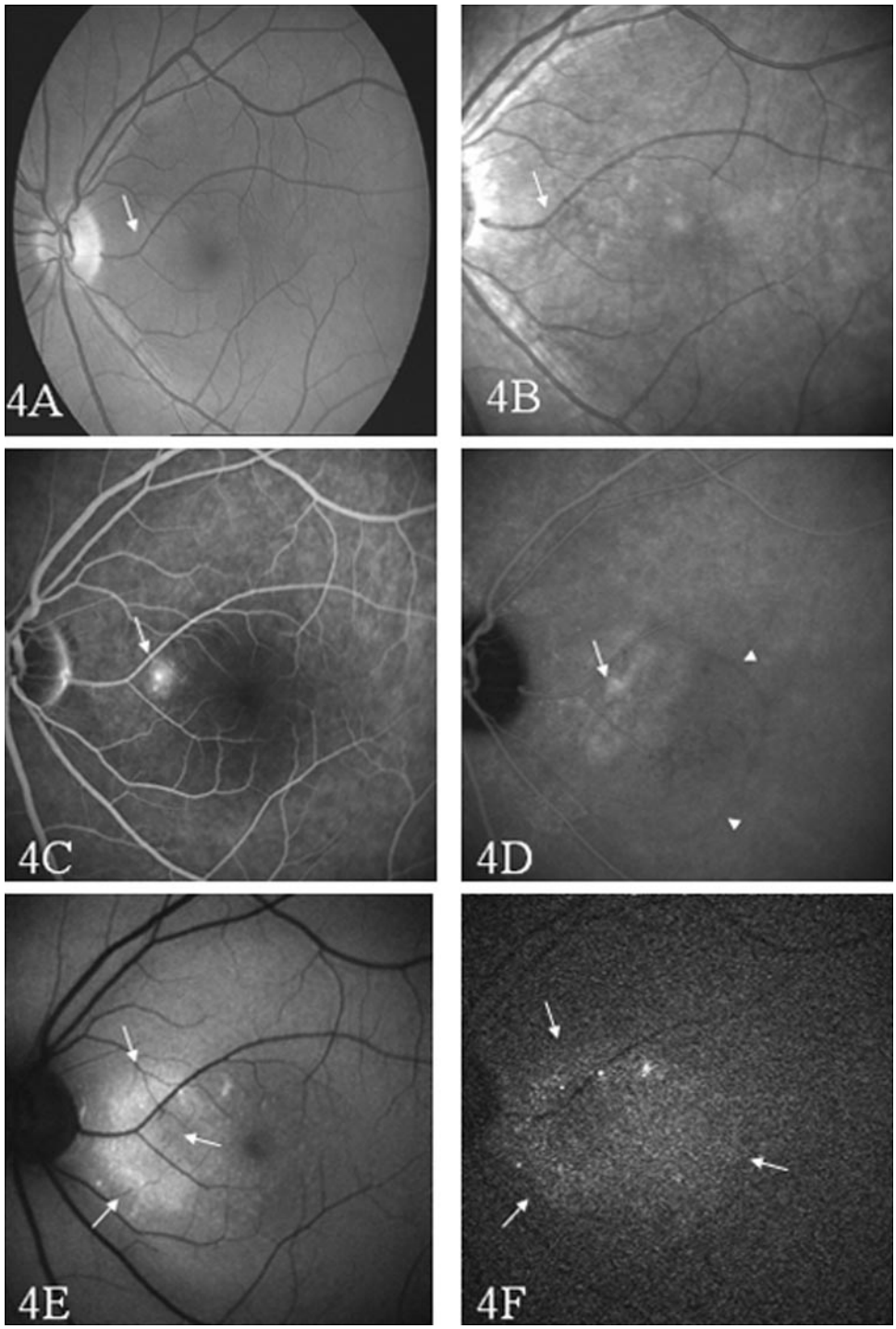

FIGURE 4. Case 4. Patient with central serous choroidopathy. (**A**) Fundus photograph showing subretinal exudate nasal to the fovea (*arrow*). (**B**) NIR reflectance image. There is no increased NIR reflectance that corresponds to the exudates (*arrow*). (**C**) Fluorescein angiogram showing fluorescein leakage in a "hot spot" nasally to the fovea. (**D**) ICG angiogram, hot spot can also be observed (*large arrow*), additionally margins of the edema zone are visible (*arrowheads*). (**E**) Blue-light–excited autofluorescence shows increased autofluorescence corresponding to the subretinal exudate. (**F**) NIR fluorescence showing an increased signal corresponding to the edema zone which appears to be NIR-autofluorescence.

in several cases in which NIR reflectance of pathologic lesions was in saturation, whereas other structures that reflected NIR light (Fig. 6) were not. It seemed further possible that both pseudofluorescence and autofluorescence contribute to the NIR fluorescence signal. Comparing gray-value ratios of NIR reflectance and fluorescence images indicates that part of the observed NIR fluorescence signal could derive from autofluorescence. It has to be mentioned, though, that gray-value analysis requires a correction for offset in the image to define the 0 gray value. For this purpose, the gray value of the darkest area in an image is determined and subtracted from gray values in the area of interest within the same image. Naturally, this correction for offset has a stronger influence on dark NIR fluorescence images than on bright NIR reflectance images, particularly if the offset value is high (Fig. 8). Because the NIR fluorescence signals are very weak and close to noise we are careful in the interpretation of these findings. The analysis of barrier filter transmission and output coupling mirror reflectance of the scanning laser ophthalmoscope revealed a leakage in the measured leakage deriving from sidebands of 6.2×10^{-6} for p-polarized and 6.7×10^{-6} for s-polarized laser light. As the output coupling mirror reflectance differed for s-polarized (0.32) and p-polarized (0.07) laser light, the observed leakage deriving from sidebands must consist of primarily nonpolarized laser light (Figs. 9, 10). Overall, the observed leakage is very discrete, supporting the idea that the observed NIR fluores-

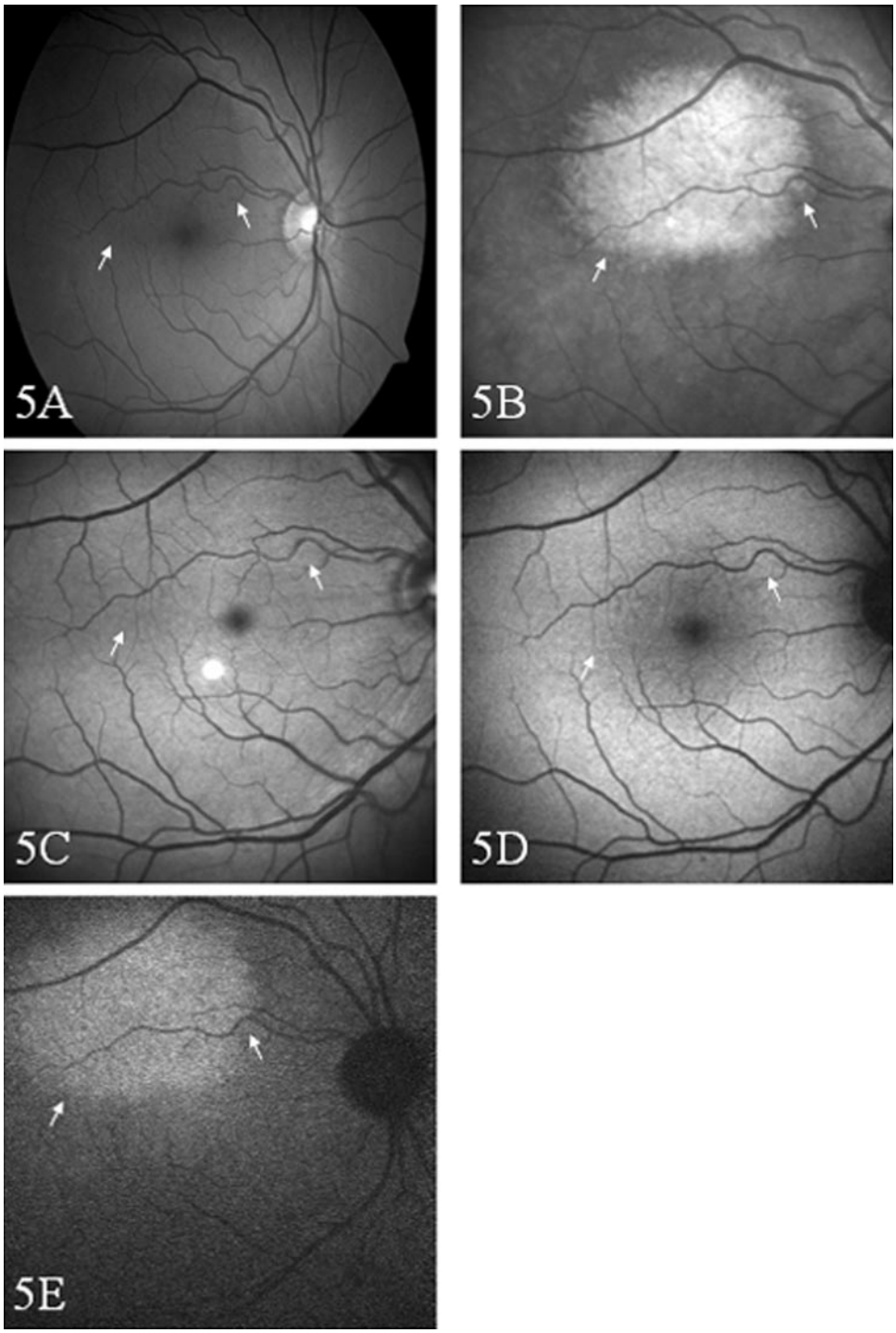

FIGURE 5. Case 5. Patient with choroidal nevus; *arrows*: nevus margin. (**A**) Fundus photograph. (**B**) NIR reflectance is increased at the nevus. (**C**) green light (red free) image, the nevus is barely visible. (**D**) Blue-light–excited autofluorescence does not show abnormal autofluorescence. (**F**) NIR fluorescence is increased corresponding to nevus and increased NIR reflectance. Angiograms were not obtained in this case.

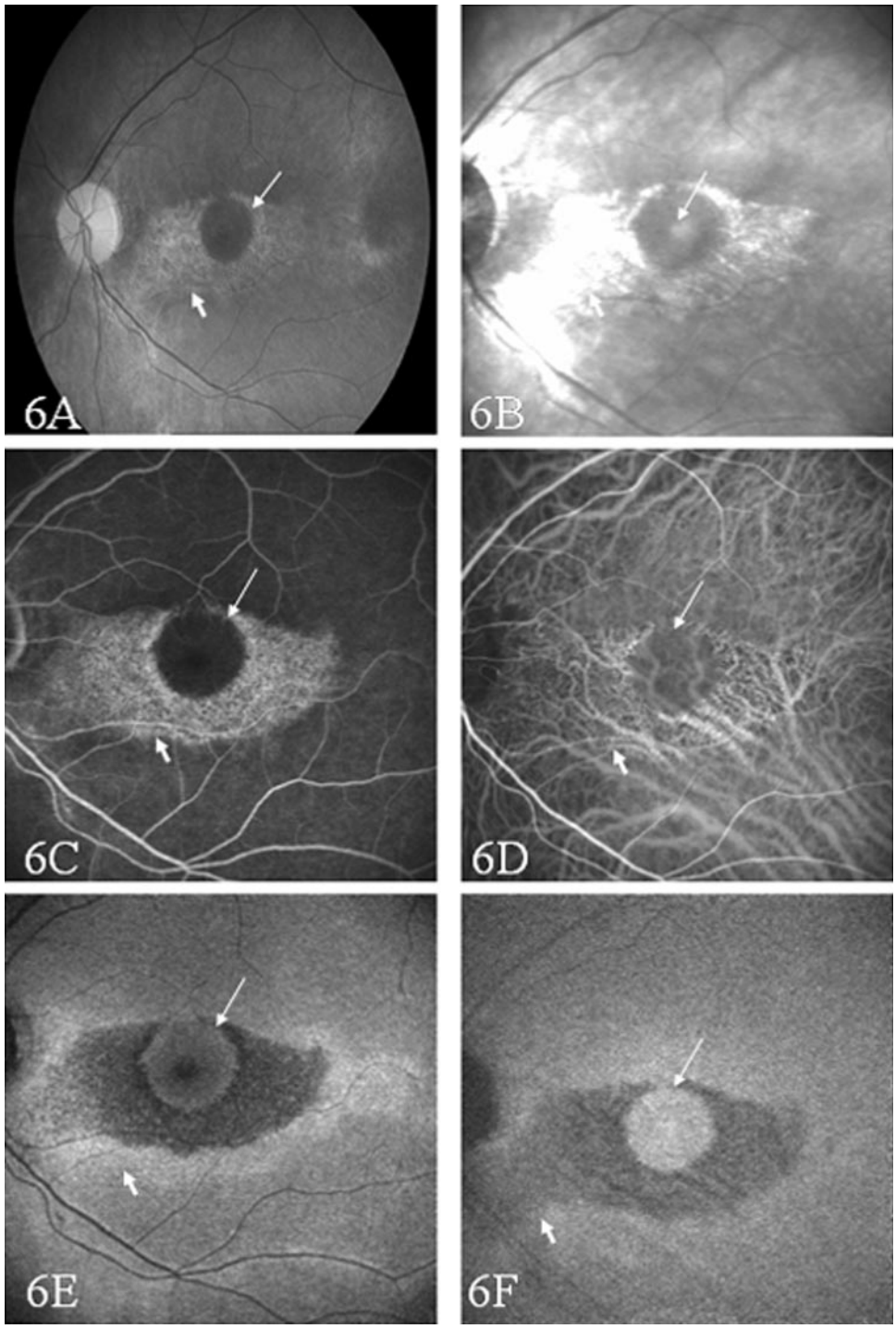

FIGURE 6. Case 6. Chloroquine maculopathy. *Arrow*: circular area of condensed pigment; *arrowhead*: area of pigment atrophy. (**A**) Fundus photograph. (**B**) NIR reflectance is increased in area of depigmentation (*arrowhead*). (**C**) Fluorescein angiogram. (**D**) ICG angiogram. (**E**) Blue-light–excited autofluorescence showing almost regular blue-light–excited autofluorescence in the circular area of condensed pigment whereas the rim of the atrophy shows increased blue-light–excited autofluorescence (*arrowhead*). (**F**) NIR fluorescence signal is strongest in the central circular area. The increased NIR reflectance does not contribute to NIR fluorescence (*arrowhead*).

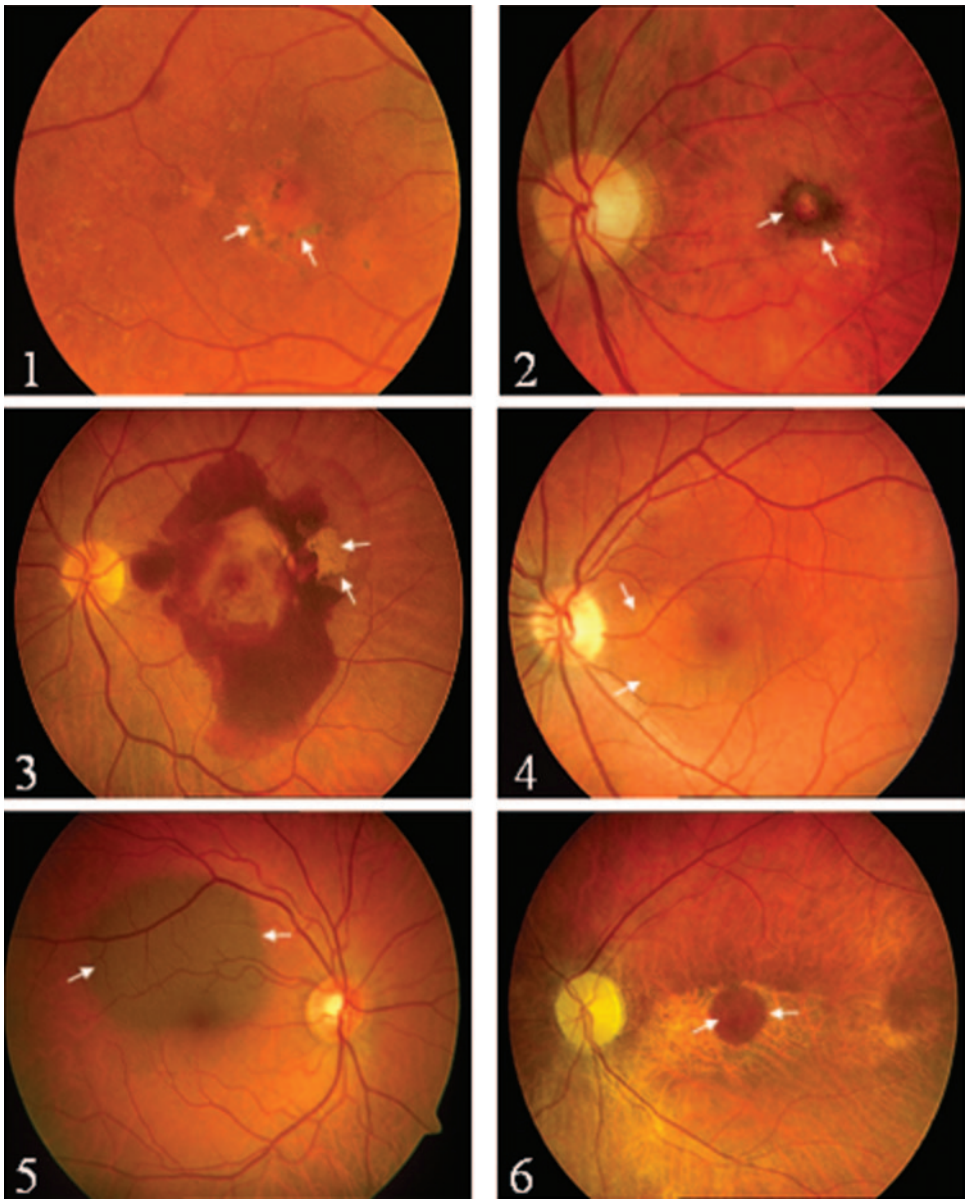

FIGURE 7. Composite of color fundus photographs showing the cases 1 to 6: Case 1. Pigment condensation in dry age-related macular degeneration/pattern dystrophy. Case 2: classic choroidal neovascularization due to age related macular degeneration. Case 3: submacular hemorrhage due to age related macular degeneration. Case 4: central serous choroidopathy. Case 5: choroidal nevus. Case 6: Chloroquine maculopathy.

cence is basically NIR autofluorescence, even if some pseudofluorescence cannot be ruled out. In four eyes with chloroquine maculopathy and chronic CSC, a weak preinjection signal could be observed, whereas the corresponding NIR reflectance image did not show increased NIR reflectance at the same fundus location. In these cases, we interpret the observed NIR fluorescence as NIR autofluorescence. The NIR autofluorescence could have been caused by accumulation of chloroquine or its degradation products. In cases of CSC, exudates from choroidal leakage like fibrin may have NIR autofluorescence properties. NIR fluorescence and increased NIR reflectance correlated in most of the patients with AMD with increased blue-light–excited autofluorescence at identical fundus locations. In contrast, NIR fluorescence due to choroidal nevi did not show increased blue-light–excited autofluorescence. Melanin appears to be the most likely candidate for increased NIR reflectance and NIR fluorescence. Obviously, the composition of pigmented RPE condensation responsible for NIR reflectance in patients with AMD is different from pigmented nevi. We speculate that lipofuscinoid fluorophores, together with pigmented melanocytes are present in these AMD cases, whereas choroidal nevi did not accumulate lipofuscin in our series. Eyes with subretinal hemorrhages showed both strong NIR fluorescence and NIR reflectance, as well as blue-light–excited autofluorescence in some cases, showing that fluorophores in degrading hemorrhages can emit light in a broad spectrum. We have also observed NIR-autofluorescence without corresponding NIR reflectance in cases of albipunctate fundus and lysosomal storage disease (data not shown). Despite the fact that acquisition of NIR fluorescence and NIR fluorescence images is simple and takes a few seconds, the relatively low incidence of NIR fluorescence we observed currently restricts the use of these imaging modalities to academic hospitals until a broader database is available. From our observation, we suggest looking for NIR reflectance and NIR fluorescence in eyes with pigmented macular lesions, CSC, and rare maculopathies.

Fundus imaging at different wavelengths complemented with NIR fluorescence– and blue-light–excited autofluorescence imaging using modern scanning laser ophthalmoscopes

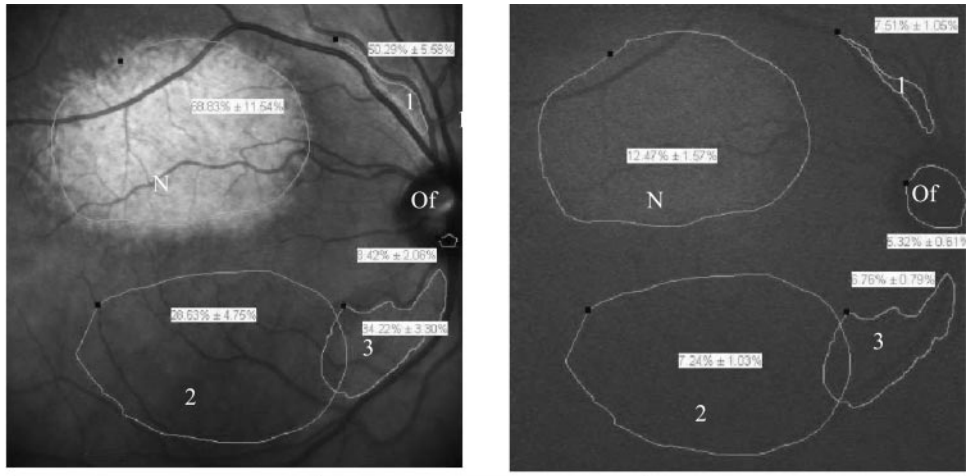

Gray value relation	IR-R (corrected for 8.4 % offset)	IR-F (corrected for 5.3 % offset)
Nevus / area 1	1.44	3.27
Nevus /area 2	2.99	3.79
Nevus / area 3	2.34	4.83

FIGURE 8. Analysis of gray-value relation between NIR reflectance image (*top left*) and NIR fluorescence image (*top right*) in case 5. The mean gray value of the nevus area (N) was compared to the mean gray value of three reference areas (1–3), corrected for the offset (Of). The gray values with SD are shown in the boxes. Data beneath images show higher gray-value relations for NIR fluorescence image compared to the NIR reflectance image, indicating that NIR-autofluorescence is contributing to the signal.

reveals a pattern of signals showing variations depending on the underlying disease. In dermatology, NIR spectroscopy of skin lesions has been used to differentiate various lesions.[12] If we can correlate histologic and spectrophotometric analysis of fundus changes with the multiwavelength imaging pattern, this noninvasive in vivo analysis of fundus changes could potentially help to discriminate between subretinal materials. For this purpose, it would be helpful if manufacturers of scanning laser ophthalmoscopes improved their products to allow direct comparison of laser intensities by supplying absolute values when comparing imaging modalities at various wavelengths.

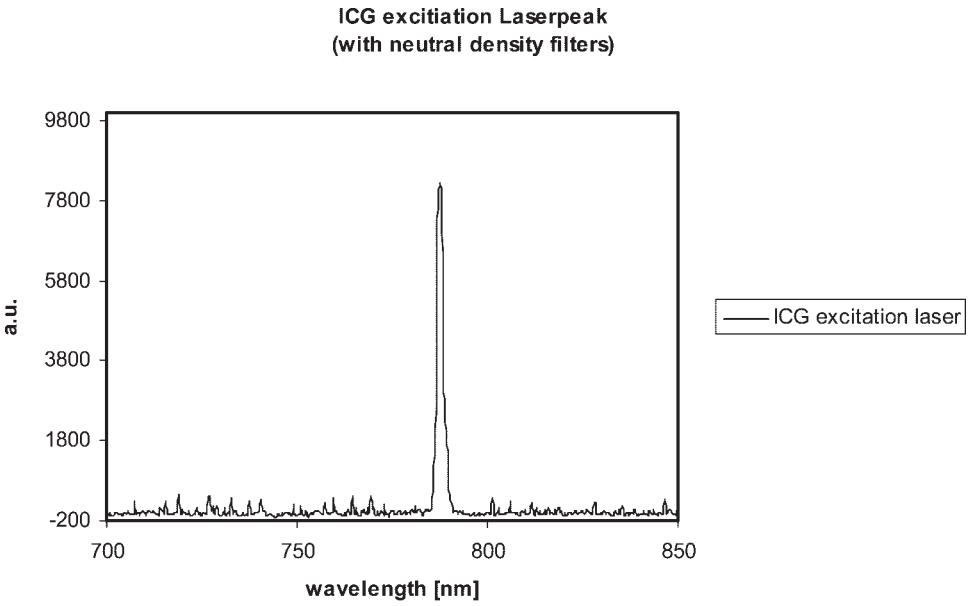

FIGURE 9. Spectrometer analysis of NIR fluorescence diode laser emission. The laser power was reduced by a series of gray filters (transmission 1.4×10^{-4}). The laser peak is detected at 787 nm without sideband emissions. *x*Axis: wavelength in nanometer; *y*-axis: laser power in arbitrary units.

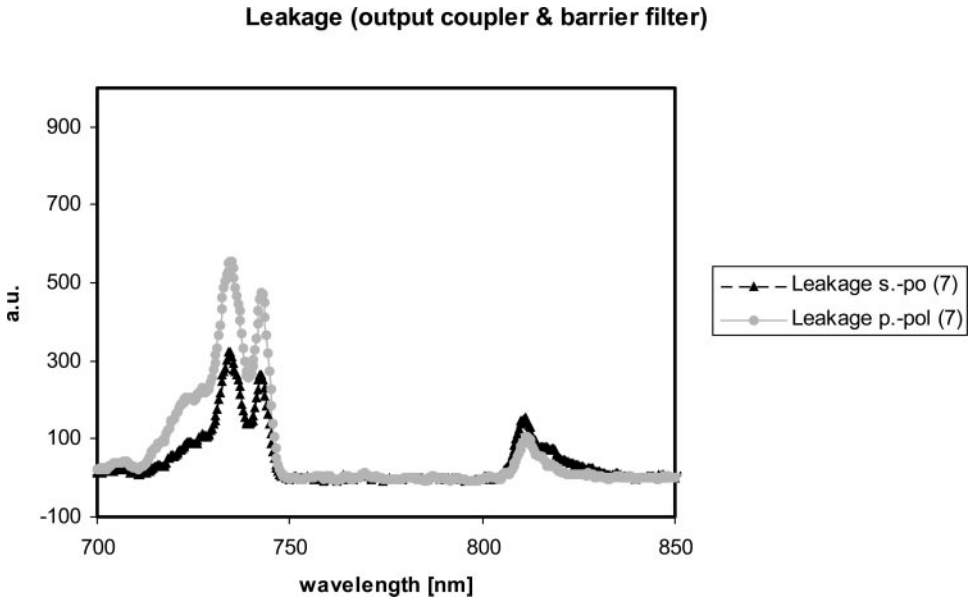

FIGURE 10. Leakage of the HRA imaging system combining barrier filter leakage and output coupler reflectance. Although the laser peak is completely suppressed, there is some sideband emission in the range of 6.2×10^{-6} (p-polarized) and 6.7×10^{-6} for s-polarized laser light measured at the standard laser power (switch position 7). *x*-Axis: wavelength in nanometers, *y*-axis: leakage in arbitrary units.

Acknowledgments

The authors thank Joerg Fischer, PhD, from Heidelberg Engineering, Dossenheim, Germany, for technical assistance, valuable discussion, and advice and Geoffrey Arden for revising the use of English in our manuscript.

References

1. Delori FC. Spectrophotometer for noninvasive measurement of intrinsic fluorescence and reflectance of the ocular fundus. *Appl Opt*. 1994;33:7439–7452.
2. Bellmann C, Holz FG, Schapp O, Völcker HE. Topographie der Fundusautofloureszenz mit einem neuen konfokalen Scanning-Laser-Ophthalmoskop. *Ophthalmologe*. 1997;94:385–391.
3. Solbach U, Keilhauer C, Knabben H, Wolf S. Imaging of retinal autofluorescence in patients with age-related macular degeneration. *Retina*. 1997;17:385–389.
4. Bindewald A, Schmitz-Valckenberg S, Jorzik JJ, et al. Classification of abnormal fundus autofluorescence patterns in the junctional zone of geographic atrophy in patients with age related macular degeneration. *Br J Ophthalmol*. 2005;89:874–878.
5. Piccolino FC, Borgia L, Zinicola E, Iester M, Torrielli S. Pre-injection fluorescence in indocyanine green angiography. *Ophthalmology*. 1996;103:1837–1845.
6. Weinberger AWA, Kirchhof B, Mazinani BE, Schrage NF. Persistent indocyanine green (ICG) fluorescence 6 weeks after intraocular ICG administration for macular hole surgery. *Graefes Arch Clin Exp Ophthalmol*. 2001;239:388–390.
7. Ashikari M, Ozeki H, Tomida K, Sakurai E, Tamai K, Ogura Y. Retention of dye after indocyanine green-assisted internal limiting membrane peeling. *Am J Ophthalmol*. 2003;136:172–174.
8. Elsner AE, Burns SA, Weiter JJ, Delori FC. Infrared imaging of sub-retinal structures in the human ocular fundus. *Vision Res*. 1996;1:191–205.
9. Sautter H, Lüllwitz W, Naumann G. Infra red photography in the differential diagnosis of suspicious pigmented fundus changes. *Klin Monatsbl Augenheilkd*. 1974;164:597–602.
10. Elsner AE, Burns SA, Delori FC, Webb RH. *Quantitative Reflectometry with the SLO.* Berlin: Quintessenz-Verlag; 1990:109–121.
11. von Rückmann A, Fitzke FW, Bird AC. Distribution of fundus autofluorescence with a scanning laser ophthalmoscope. *Br J Ophthalmol*. 1995;79:407–412.
12. McIntosh LM, Summers R, Jackson M, et al. Towards non-invasive screening of skin lesions by near infrared spectroscopy. *J Invest Dermatol*. 2001;116:175–181.